Title

Analysis of NOx Formation in a Hydrogen-Fueled Gas Turbine Engine

Journal

Journal of Engineering for Gas Turbines and Power, 131(3)

ISSN

0742-4795

Authors

Therkelsen, Peter
Werts, Tavis
McDonell, Vincent
et al.

Publication Date

2009-05-01

DOI

10.1115/1.3028232

Proceedings of ASME Turbo Expo 2008: Power for Land, Sea and Air
GT2008
June 9-13, 2008, Berlin, Germany

GT2008-50841

ANALYSIS OF NO_X FORMATION IN A HYDROGEN FUELED GAS TURBINE ENGINE

Peter Therkelsen, Tavis Werts, Vincent McDonell and Scott Samuelsen

UCI Combustion Laboratory
University of California, Irvine, 92697-3550

ABSTRACT

A commercially available natural gas fueled gas turbine engine was operated on hydrogen. Three sets of fuel injectors were developed to facilitate stable operation while generating differing levels of fuel/air premixing. One set was designed to produce near uniform mixing while the others have differing degrees of non-uniformity. The emissions performance of the engine over its full range of loads is characterized for each of the injector sets. In addition, the performance is also assessed for the set with near uniform mixing as operated on natural gas. The results show that improved mixing and lower equivalence ratio decreases NO emission levels as expected. However, even with nearly perfect premixing, it is found that the engine, when operated on hydrogen, produces a higher amount of NO than when operated with natural gas. Much of this attributed to the higher equivalence ratios that the engine operates on when firing hydrogen. However, even at the lowest equivalence ratios run at low power conditions, higher NO was observed. Analysis of the potential NO formation effects of residence time, kinetic pathways of NO production via NNH, and the kinetics of the dilute combustion strategy used are evaluated. While no one mechanism appears to explain the reasons for the higher NO, it is concluded that each may be contributing to the higher NO emissions observed with hydrogen. In the present configuration with the commercial control system operating normally, it is evident that system level effects are also contributing to the observed NO emission differences between hydrogen and natural gas.

INTRODUCTION

Gas turbine engines designed to operate on various fuel stocks are available commercially. Most commonly natural gas and liquid kerosene are used to fuel gas turbine engines.[1] Opportunity fuels such as gases produced from landfills and anaerobic digesters have become popular recently due to both increased criteria pollutant control that restricts the ability to simply vent these gases to the atmosphere and the economic benefits of their conversion to useful electricity and waste heat.[2] Often, the quantities of these fuels available warrants relatively small engines. As a result, engines producing 30 to 250 kW ("microturbines" or MTGs) are of interest for many of these applications. These fuels typically contain large quantities of carbon dioxide and nitrogen compared to natural gas. Studies of MTGs operated with these low energy-containing fuels have shown that emission levels of criteria pollutants including carbon monoxide and oxides of nitrogen are influenced by the same control techniques developed for engines fueled with natural gas.

With economic and political drivers in place, hydrogen has seen an increase in applications to a wide range of power generation devices. These include both large-scale gasification/power generation plants and distributed generation devices. Historically hydrogen has seen limited use in gas turbine engines though research has been documented.

The National Advisory Committee for Aeronautics conducted tests of a kerosene-fueled engine with hydrogen.[3] These tests were conducted with an aero-engine onboard an aircraft at altitude. These tests focused on engine efficiency and relight abilities with regards to altitude. The hydrogen engines were better able to maintain a reaction and restart after blow out at high altitudes. The superior combustion properties of hydrogen were exploited to reduce the combustor length by 40 percent compared to the kerosene combustor.

Nomura, et al. conducted atmospheric testing of a liquid fired can combustor with hydrogen.[4] These tests utilized a 202kW gas turbine combustor. The kerosene fuel supply system was removed and a hydrogen flow metering system was installed. Data were obtained on pressure losses of the fuel system, ignition performance, temperature distributions, combustion efficiency, liner wall temperature distributions, NO_x emission levels, noise levels and operating performance. The conversion from liquid fuel system to hydrogen was not found to be complicated. A swirler type injector as well as an angled cone injector with small holes was used. The cone type injector was found to degrade quickly due to its protrusion into the combustion chamber. Combustor efficiency was not

reduced with hydrogen operation. While noise levels did not increase with hydrogen, emissions of NO_x were found to be greater than those produced with kerosene combustion. To reduce NO_x emission levels new fuel nozzles were recommended.

Pratt and Whitney Canada tested two liquid fired can combustors in laboratory bench tests with hydrogen.[5] This work extended that done by Nomura by elevating the pressure of the combustors up to 1.0MPa. For each combustor liner two different types of injectors were used. The research showed that a liquid fired can combustor could be retrofitted with a different injector to operate with hydrogen. Issues of uneven liner temperatures and increased NO_x levels compared to liquid Jet-A operation were noted. The benefits of increased combustion efficiency and ease of ignition made were also seen. Liner geometry modifications to reduce reaction zone temperatures and residence times were suggested as next steps to reduce NO_x emissions.

The utilization of pure hydrogen in a gas turbine poses certain challenges that have been outlined.[6,7] The nature of hydrogen to react easily and quickly have led to concern of flashback and autoignition for premixed systems. In addition hydrogen reacts on average 126K hotter than natural gas for an equal equivalence ratio.[7] Emissions of NO_x from a stoichiometric hydrogen reaction have been shown to exceed current regulatory limits.[6]

Measurements of NO have been reported for a retrofitted natural gas MTG operated on hydrogen.[7] The emission levels were found to be 10 to 100 times greater than those produced by the commercial MTG operating on natural gas. Equivalence ratio and fuel/air mixing were both shown to play a roll in the generation of relatively high NO levels. This study went on to conclude that further improved mixing should result in further NO emissions reductions. The present work extends this earlier work by achieving the refined mixing, characterizing the subsequent emissions and also discusses in detail the NO emissions characteristics observed.

APPROACH

To accomplish this, the following steps are taken:

- Characterize three unique injection systems for fuel/air mixing at various power loads.
- Operate the MTG with each of the injection systems over the full load range measuring performance characteristics and stack emission levels.
- Operate the MTG on natural gas using the injector set resulting in the lowest emissions when operated on hydrogen.
- Evaluate the effect of residence time, chemistry, and overall combustor configuration on the relative levels of NOx formation observed.
- Operate the MTG on a varying mixture of natural gas and hydrogen at full load to measure the effects on stack emission levels.

EXPERIMENT

A brief overview of the experimental apparatus and numerical methods used in this study is provided below.

Capstone C60 Microturbine

The Capstone C60 is a commercially available natural gas fueled recuperated Brayton cycle engine. It has been extensively studied when operating with natural gas as well as other fuels such as digester gas and landfill gas.[2,7,8]

Air enters the C60 and is passed through a recuperator. It is then compressed via a radial compressor to a pressure of approximately four atmospheres. The air enters the engine in one of three ways; as primary zone combustion air or as part of two dilution zones. The manufacturer quantified this flow split, allowing calculation of combustor primary zone equivalence ratio. The quantified flow split information is proprietary. The combustor, diagramed in Figure 1, contains six injectors tangentially inserted on two planes. The six injectors are fuel staged throughout the operational load of the engine. All injectors flow air regardless of fuel flow. The first plane contains two injectors. These injectors are always fueled during engine operation. The remaining four injectors are located on the second plane. These injectors are fueled based upon engine power demand. This fuel staging creates a quench effect when some injectors are not fueled. Previous work[8] showed this effect will aid in the formation of carbon monoxide when the engine is fueled with natural gas. Relatively cool air enters the combustion chamber through these injectors such that the injectors act as large scale dilution ports.

Carbon monoxide formation was not a problem with hydrogen operation in this experiment due to the lack of carbon in the system. Control of the primary zone fueling was necessary however to ensure all six injectors were equal in their contribution to the combustion reaction. Having six equal injectors over the full power load of the engine allowed for better comparisons of equivalence ratio and emissions.

It is noted that the engine control system is working from set points on turbine exhaust temperature and shaft speed. The engine varies shaft speed to meet the power demand and it adds fuel accordingly. The exhaust temperature limit point precludes overheating of the engine and will limit fuel flow and therefore power if necessary.

Simultaneous onboard and external data acquisition systems provided engine operational data during testing. As part of the C60 fuel staging, engine shaft speed and airflow data were recorded. Fuel flow rate was measured externally to the engine using a positive displacement gas meter (Roots). Delivered power from the engine as well as fuel pressure and temperature were also measured external to the engine. Ambient conditions were recorded as well.

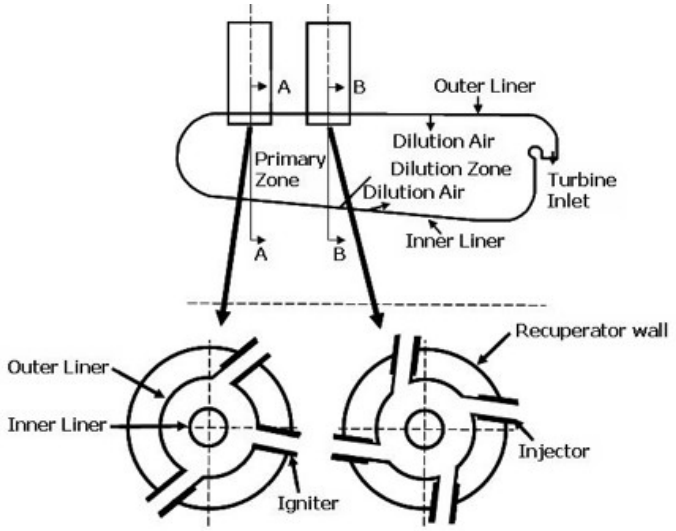

Figure 1: C60 Combustor Outline with Injector Plane Cross Section.

Emissions Console

A gas analyzer (Horiba PG 250) was used to measure emission levels. A continuous gas sample was drawn from the MTG exhaust stack with a vacuum pump connected to a stainless steel probe. The analyzer draws from this gas line and measures the stream for levels of NO, CO, CO_2, SO_2 and O_2. At 30-second intervals these data were electronically logged. The analyzer was zeroed and spanned before each test. Drift checks showed less than 1% variation for all channels.

Injector Test Rig

An atmospheric test rig was used to simulate airflow distribution to a single injector. The C60 utilizes tangential injection that produces unique flow fields that are inherently asymmetric. By using the actual C60 injector bellows assembly the complex series of airflow turns in an actual engine is properly simulated. A more detailed description of the injector test rig operation is documented in previous work.[7]

Gas Chromatograph

An SRI gas chromatograph (GC) was used to measure mixing profiles generated by the hydrogen injectors. The GC was calibrated using a certified sample gas mixture to ensure its accuracy. The GC was calibrated and checked before each test with drift remaining under 1 percent during all testing. Further details about the operation of the GC are found in previous work.[7]

Chemical Kinetics Code

CHEMKIN[9] was used to model kinetics behavior using the GRI 3.0 mechanism[10] as well as that of Konnov.[11] While other mechanisms[12] are available that are more directed at modeling the hydrogen/air reaction, for the present work it was helpful to use a common mechanism that can simulate both hydrogen and methane air reactions. Both mechanisms used have low temperature NO formation reactions that are investigated as part of the study.

MODIFIED INJECTOR DESIGN

Several modifications were made to the commercial C60 injector (Figure 2) to ensure safe, stable operation of the engine when operated on hydrogen.[7]

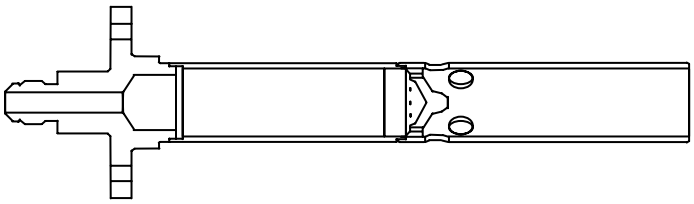

Figure 2: Fuel Injector, OEM Natural Gas C60 Injector

Designs to generate differing fuel/air profiles for a given equivalence ratio were developed. To help mitigate flashback concerns,[7] the fuel injection point within the mixing tube was moved closer to the injector exit plane, downstream of where air enters the injector. The commercial C60 injectors utilize a fuel distributor located approximately half way down the mixing tube. Moving the fuel entry point forward nearly 90% of the injector length, the total volume of the injector exposed to a combustible mixture was significantly reduced. By introducing the fuel to the injector downstream of where air enters the injector, the possibility of a combustible mixture located in a wake or other aerodynamic feature associated with air entry into the injector was also reduced.

An insert was placed into the injector exit plane to further reduce the likelihood of flashback. The insert extends inside the injector from the exit plane to the point of fuel injection. This insert contains one 1.78 cm diameter center hole in which all of the fuel and most of the air is mixed and released to the combustion chamber. The remainder of the injector air is distributed to 6 cooling slots that run along the inner wall of the injector. These slots comprise about 17% of the total injector airflow area.

The hydrogen injectors are designed to operate fuel lean to reduce reaction temperature and minimize pollutant emissions. For a given equivalence ratio, hydrogen reacts at a temperature approximately 126K higher than methane. However, the wide hydrogen stability limits allow the reaction to be sustained at much lower equivalence ratios (and correspondingly lower temperatures) than natural gas (as low as 0.09 vs 0.48 for natural gas).[7] To take advantage of this attribute, the air flow into the injectors was increased, resulting in equivalence ratios ranging from 0.21 to 0.7 across the 0-60kW power load range.

Three injector sets were fabricated, each designed to flow the same amount of air and fuel across the power load range, but providing differing degrees of fuel/air mixing to allow the

influence of mixing on emissions to be studied. Each design releases fuel to a mixing length via a 6.35mm tube. In one case the fuel enters the air stream co-flowing with the air. This injector type is denoted as an "axial injector" (Figure 3).

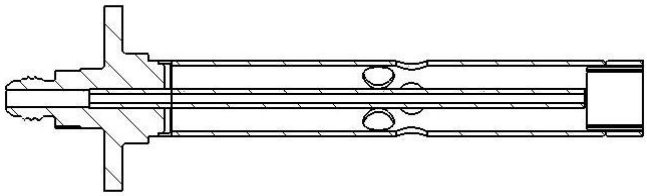

Figure 3: Fuel Injector, Axial Hydrogen Injector

Two injectors feature two rows of six one-millimeter holes on the side of the capped tube which provide radial fuel injection. The two radial injectors differ in the mixing length afforded to the fuel/air mixture prior to injection into the combustor. The first has a mixing length of 19mm (the same length as the axial injector) and is labeled the "radial injector". The third injector is called the "early radial injector" due to its 63.5mm mixing length. The two radial injectors are shown in Figure 4 and Figure 5.

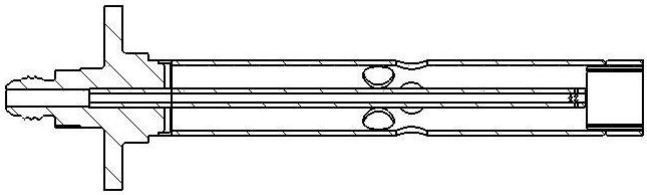

Figure 4: Fuel Injector, Radial Hydrogen Injector

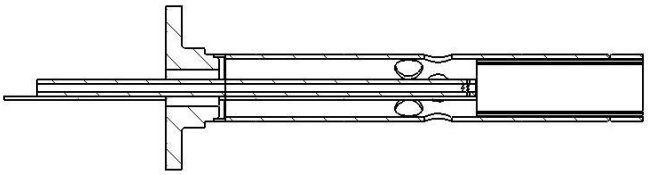

Figure 5: Fuel Injector, Early Radial Hydrogen Injector

MODIFIED INJECTOR MIXING RESULTS

The fuel distribution across the exit plane was measured for each injector type. Engine conditions were approximated at 1 atm and 300 K by matching momentum. Three power settings, 5kW, 30kW and 60kW, were tested. Measurements were taken as a single line across the diameter of the injectors.

Measurements of hydrogen concentration were taken by GC and reported as volumetric percentages. These volumetric concentrations for all three injector types can be seen in Figure 6. These volumetric concentration values were then equated to equivalence ratio, shown in Figure 7. In both graphs the x-axis indicates location along the injector exit diameter with 0.0 being the middle of the injector. All three injector exit planes are 17.78mm in diameter. Lines indicating upper and lower flammability limits are included in Figure 7 for reference.[13]

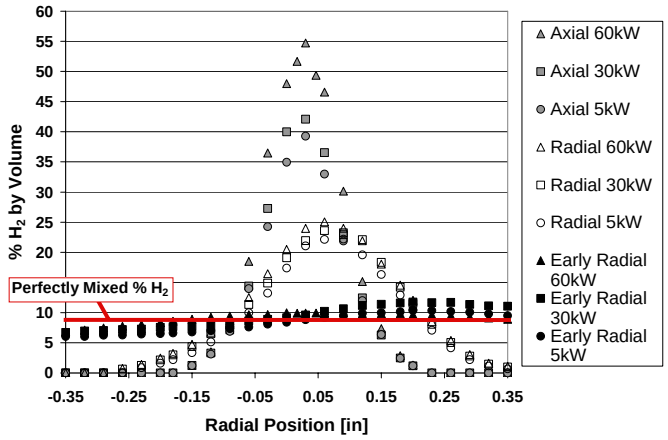

Figure 6: Radial, Axial and Early Radial Hydrogen Injector Mixing Profiles for Multiple Power Loads, Volumetric Concentration Comparison

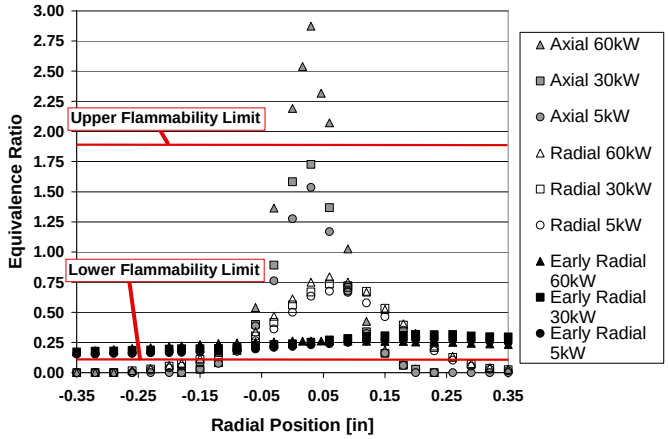

Figure 7: Radial, Axial and Early Radial Hydrogen Injector Mixing Profiles for Multiple Power Loads, Equivalence Ratio Comparison

Integration of the measured profiles show less than 3% variation of total hydrogen between radial and axial hydrogen injectors for each power load tested, indicating consistent fuel flows for each configuration. The asymmetry of the concentration peaks has been observed in other tests[8] of OEM Capstone injectors and is due to the complex airflow that develops in the injector feed annulus.

Each injector type creates a unique mixing profile as seen in Figure 6 and Figure 7. The axial injector produces peaks between 55 and 39 percent for the different power loads. The radial injector produces a maximum concentration of 25 percent at 60kW and 22 percent at 5kW. In addition,

differences as a function of load are reduced with the radial injector. The early radial injector produced the most uniform concentration profile of the three. The profile still exhibits the modest asymmetry, but approaches uniform mixing (Figure 6). The early radial injector also exhibits smaller differences as a function of load.

When examined as a function of equivalence ratio the axial injector creates a mixture at 60kW that exceeds the upper flammability limit. This indicates that a diffusion flame will be produced, resulting in high reaction temperatures and high NO_x formation rates. The radial or early radial injector does not exceed the upper flammability limit. Both the axial and radial injectors do not have a combustible mixture present at the injector walls by design. The early radial injector does have a combustible mixture present at the walls, which could be a concern from a flashback viewpoint.

ENGINE OPERATION AND EMISSIONS RESULTS

The MTG was started and operated on pure hydrogen for all tests. Previous work conducted accounts for start up procedures and experiences.[7] Four tests each were conducted for the axial, radial and early radial hydrogen injectors. These tests were done at slightly different ambient temperatures as summarized in Table 1, Table 2 and Table 3.

Table 1: Test Numbers and Ambient Temperatures [K] for Axial Hydrogen Injectors

	Axial 1	Axial 2	Axial 3	Axial 4
Ambient Temperature	292.6	297.3	293.7	293.2

Table 2: Test Numbers and Ambient Temperatures [K] for Radial Hydrogen Injectors

	Radial 1	Radial 2	Radial 3	Radial 4
Ambient Temperature	292.6	291.7	291.3	290.7

Table 3: Test Numbers and Ambient Temperatures [K] for Early Radial Hydrogen Injectors

	Early Radial 1	Early Radial 2	Early Radial 3	Early Radial 4
Ambient Temperature	292.4	291.1	291.7	292.2

Calculation of equivalence ratio requires knowledge of the engine air flow. Capstone provided an equation relating engine shaft speed and turbine exit temperature to total air flow. This equation was developed with the commercially available natural gas engine. Tests conducted with hydrogen demonstrated that, for all power loads, shaft speed and turbine exit temperature values were the same as those with natural gas fueled engine,[7] confirming applicability of the expression for the current work. Primary zone airflow was determined from this total air flow. Engine airflow splits for the natural gas engine were provided. By creating ratios of effective area measurements for natural gas injectors to hydrogen injectors new primary zone air splits were calculated.

Emissions were measured from the engine operated using each injector set run over the full operational load range with hydrogen. For each injector four separate tests were conducted to ensure repeatability. NO and O_2 emissions levels were measured. Emission values of NO were corrected to 15% O_2. A correlation of NO to NO_x can be found in other work.[7]

Figure 8 shows the NO emission levels as a function of load for each injector type. Each injector type produces a near linear relation between NO emission and power load. For all power settings the axial injector produces the most NO with the radial and early radial producing less each. The slope of the emissions vs load line differs for each injector, ordered by axial, radial, and early radial. At a power level of 5kW both the axial and radial injectors produce just below 70ppm NO. The early radial injectors produce just over 25ppm NO at 5kW. At the full load point of 60kW the axial injectors produce between 313-360ppm of NO depending upon ambient temperature. The radial injectors produce 243-269ppm NO at 60kW. The early radial injectors produce between 92-110ppm NO at 60kW.

The effect of ambient temperature has been discussed in earlier experiments with hydrogen MTGs.[7] The effects of ambient conditions are most noticeable when the engine is operated with the axial injectors. Ambient temperature effects are noted with the radial and early radial injectors but to a lesser degree.

A relation between emissions and equivalence ratio is shown in Figure 9. For all injector types equivalence ratio varies between 0.2 and 0.7 for hydrogen. A red vertical line has been inserted into Figure 9 to indicate the lean flammability limit of hydrogen. As equivalence ratio decreases NO emission decreases for all injector types. Similar trends between NO emissions and power load are seen between NO emissions and equivalence ratio.

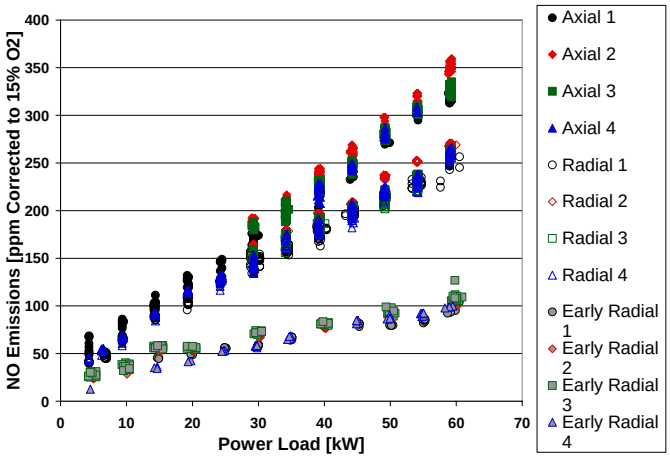

Figure 8: Axial, Radial and Early Radial Injection NO Emissions vs. Power Load (Full Load Range)

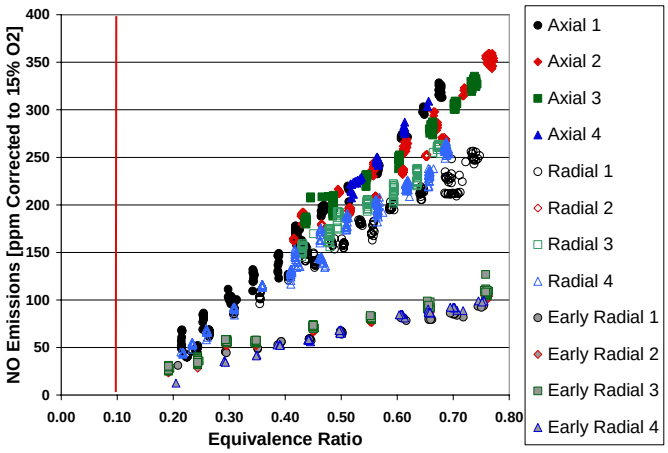

Figure 9: Axial, Radial and Early Radial Injector NO Emissions vs. Equivalence Ratio (Full Load Range)

Axial 1, Radial 1 and Early Radial Test 1 can be directly compared for their levels of NO. The three sets of data have been taken with an ambient temperature difference of less than 0.4%. A distinct correlation between injector type (i.e., fuel mixing) and NO emission level can be seen. At an equivalence ratio of 0.7 a NO emission jump of 39% is seen between the axial and radial injectors. A 169.5% variation is seen between the early radial and radial injector. This extreme jump in emission level indicates a strong relation of NO emission level to fuel/air mixing.

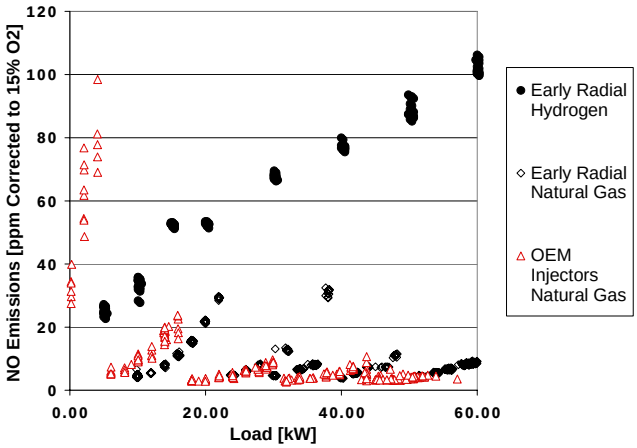

Figure 10: NO Emissions for Early Radial Injector Operated on Hydrogen and Natural Gas

The early radial injectors were fueled with natural gas and emission levels of NO taken in order to confirm that differences between the mixing for the OEM injector and the early radial injectors were not giving rise to significantly different NOx emissions. This injector was chosen because it produced a near uniform mixing profile (see Figure 6). In order to maintain stability with natural gas operation, the engine *must be* fuel staged. As power load increased the number of injectors that were fueled increased. Hydrogen operation does not require fuel staging. The natural gas operation produced emissions of NO between 3.5ppm and 31ppm. The results are seen in Figure 10. Note that the staging occurs at different power loads for the two fuels. This is attributed to differences in the flame temperatures and inlet temperatures during the tests.

Overall the geometry changes made to the fuel injection system did not affect the engine's performance when fueled with natural gas. For all power settings the engine fueled with hydrogen produced significantly higher NO than it does when fired on natural gas.

To help further understand the behavior of the engine as fuel type is changed, additional tests were run at full load using a varying mixture of natural gas and hydrogen demonstrate an exponential increase in NO emission as the percentage of hydrogen increases. Shown in Figure 11 the results show that there is a substantial jump in NO production from 60% hydrogen to 100% hydrogen.

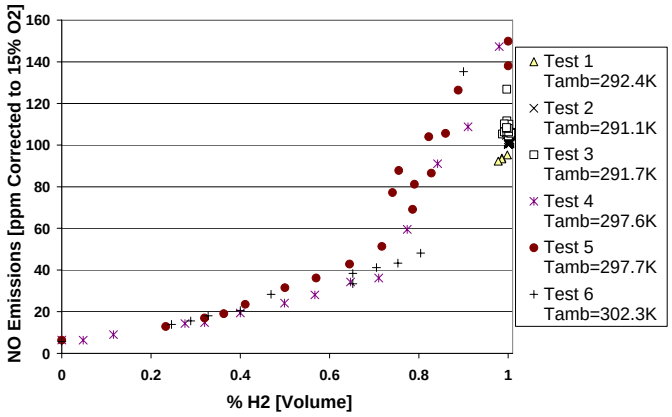

Figure 11: NO Emissions for Early Radial Injectors Operated on a Mixture of Hydrogen and Natural Gas

DISCUSSION

Though the increase of NO emission from a retrofitted gas turbine is consistent with historical work[3,5] an understanding of why an increase is seen is desired. In the present case, two different issues are noted. First, at full power, the engine primary zone equivalence ratio when operated on hydrogen is much higher than it is for natural gas. This leads to significant thermal NO formation. However, because of the turbine exit temperature limit point, this presents a paradox regarding heat transfer within the system because the exhaust must reach the relatively cool turbine exit temperature regardless of the temperature it starts from in the primary zone. Apparently, for hydrogen, a much higher primary zone temperature results than it does for natural gas. Second, even at the very low equivalence ratios found at low power, the NO levels are still higher than they are for natural gas. Four potential effects

leading to higher NO emissions in these two cases are explored in this section.

MTG Control Strategy

The MTG used in this experiment controls the amount of fuel added to the reaction based on the turbine exit temperature. At full load on hydrogen, running at an equivalence ratio of 0.70 (based on metered air and fuel flows), the flame temperature in the combustor primary zone will be several hundred degrees higher than the equivalent full load condition running on natural gas at an equivalence ratio of 0.49. This higher flame temperature explains the much higher overall NO emission at full load as a result of the thermal formation of NO in the combustor. What is perplexing is how the exhaust gases for hydrogen can be so hot in the primary zone compared to natural gas, yet still reach the same turbine exit temperature set point. Several experiments were done to try to explain how the temperature between the combustor and the turbine exit could vary so greatly for the two fuels. At this point, additional information regarding relative heat transfer to the liner is needed to fully explain what is going on.

At the low power end of the spectrum, the equivalence ratio is relatively low and the apparent reaction temperatures are also low. As a result, other factors may be contributing to the differences in NO emission.

Effect of Residence Time

The MTG used in this study was designed to operate on natural gas. It is surmised that the combustion chamber of the original engine has been optimized to minimize pollutant formation when operated on natural gas. This optimized configuration may lead to higher NO emission levels when the engine is run with hydrogen. Previous work has indicated that gas turbines operated on hydrogen could use a shorter combustor compared to those used for conventional fuels due to the relative fast reaction rate of hydrogen.[3] Use of an oversized geometry creates an unnecessarily long residence time. To further explore this, NO formation rates were modeled at engine inlet conditions of 832.75K and 3.599atm in a simplistic single perfectly stirred reactor model. An equivalence ratio of 0.49 for methane was used to represent the 60 kW point of engine operation. Hydrogen was modeled with a 0.70 and 0.14 equivalence ratio. The 0.70 point represents the 60kW operation point measured in the operational engine with the current injector modifications while the 0.14 point represents the lowest possible equivalence ratio the engine could theoretically achieve with a complete reconfiguration of the air flow splits. Initial reactor temperatures were set to the adiabatic flame temperature levels of the corresponding fuel and equivalence ratio levels. Both the GRI 3.0 and Konnov mechanisms were used. This was done in part to help understand the sensitivity of the conclusions regarding low temperature NO formation to the mechanism used.

The results of this modeling are shown in Figure 12. Though the exact residence time of the primary zone of the combustor is not known it is estimated based upon combustor geometry to be between 7.8ms and 8.8ms over the load range of the engine. At comparable 60kW points the hydrogen reaction with an equivalence ratio of 0.70 has a greater NO formation rate for a shorter amount of time. Unless a combustor could be made that would terminate a reaction in under a millisecond at this equivalence ratio large amounts of NO will be formed. The hydrogen reaction with an equivalence ratio of 0.14 however shows that, at a reduced equivalence ratio, the magnitude of the NO formation rate can be reduced. The length of time during which NO is being formed however is significantly larger. A short yet realistic combustor could take advantage of this longer reaction time and prematurely quench NO formation. By shortening the combustor length and lowering equivalence ratio the formation of NO in a hydrogen-fueled MTG can be reduced.

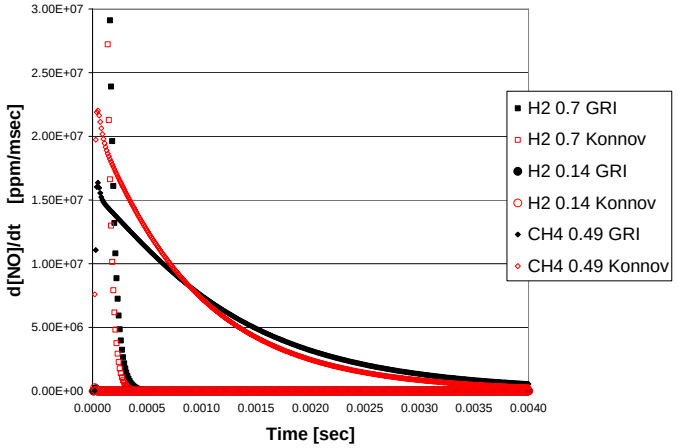

Figure 12: NO Formation Rate for Methane and Hydrogen at Given Equivalence Ratios

NO is formed considerably faster with hydrogen at operational engine condition equivalence ratio of 0.70 than when operating on methane at an equivalence ratio of 0.49. In addition, the equilibrium amount of NO produced in the hydrogen engine is 2.3 times higher than that of methane at an equivalence ratio of 0.49. By dropping the equivalence ratio of hydrogen to 0.14 the initial formation rate of NO drops well below that for methane at 0.49. The equilibrium value of NO from hydrogen at an equivalence ratio of 0.14 is 15 times less than that from methane at 0.49.

From this analysis, two possible NO reduction methods are apparent. Clearly, lowering the equivalence ratio reduces both the formation rate and total amount of NO formed. In addition if the residence time during which species exist at elevated temperatures is reduced the formation of NO could be extinguished before reaching equilibrium. However, the high NO levels measured from the engine operated on hydrogen at an equivalence ratio of 0.14 observed in engine measurements (Figure 9and Figure 10) are in contrast to this simplified reactor analysis. Hence further investigation into possible NO formation paths is warranted.

NO Formation Analysis

Traditional NO formation routes including thermal, prompt and N_2O may not fully account for all NO produced in hydrogen fired systems. In addition to these pathways, as first suggested by Miller et al.[14] NNH is another intermediate species contributor to NO formation and may be important in the current system. NNH has been shown to explain discrepancies between NO concentrations from hydrogen reactions measured by laser induced fluorescence and modeling of traditional (thermal, N_2O, prompt) NO formation mechanisms.[11]

Bozzelli and Dean[15] used this idea when introducing the O + NNH = NO + NH pathway as an important part of NO production models. This pathway is shown to be an important contributor to NO_x production including cases where large concentrations of H and O molecules are present. Combustion of hydrogen and air in a gas turbine engine provides large amounts of dissociated H_2 and O_2. NNH dissociation to H and N_2 is shown to be expected under all conditions yet due to the nearly thermoneutral nature of NNH = H + N_2 at high temperatures NNH formation from H and N_2 is also rapid. Bozzelli and Dean also suggest that of the several bimolecular reactions associated with NNH the most important is that with O atoms. Additionally by appropriately adding the NNH formation reactions to a kinetics mode,l predicted concentrations of NO may be increased by an order of magnitude.

The formation of NO via the NNH pathway occurs in both hydrogen and methane flames for all equivalence ratios.[16] The amount of NO produced that is attributed to the NNH pathway however depends greatly upon temperature, equivalence ratio and pressure. Hayhurst and Hutchinson[17] are also supportive of the importance the NNH pathway plays in NO formation. Their work too shows that the NNH pathway will form NO in both hydrogen and methane flames.

NNH is also shown to be the dominant route of NO formation in systems with short residence times in the order of 1 to 25ms for all temperatures.[Error! Bookmark not defined.] For systems exceeding this residence time window NNH still plays a role in the formation of NO yet primarily at low temperatures. At higher temperatures the Zel'dovich mechanism is dominant.[17] For hydrogen/air systems Konnov, Colson and De Ruyck state the flames above 2100K are dominated by thermal NO and below that value by NNH.[16]

Low temperature shows greater sensitivity to NNH for lean flames.[16] Under fuel-rich conditions however a large discrepancy between the arrhenius plot of the third equation in the Zel'dovich mechanism (N + O_2 → NO + O) and experimental measurements of NO was found. This discrepancy is attributed to the formation of NO via the NNH pathway that is not described by Zel'dovich.[16] In fuel-rich systems an abundance of free H atoms accelerates the formation of NNH via the reaction H + N_2 = NNH.[17] Others also found that while NNH is present for all situations that during fuel-rich conditions thermal NO dominates NO formation.[16,18,19]

In addition to the arguments by Bozzelli and Dean[15] other work has shown discrepancies in the modeling of NNH NO with kinetics codes. The GRI 2.11 mechanism was shown to over predict NO levels formed due to NNH in methane flames at high pressures.[20] Simultaneously Konnov, Dyakov and De Ruyck state that the GRI 2.11 mechanism shows that NNH is a viable explanation for ppm levels of NO found in hydrogen/air flames.[11] Hughes et al. shows an improvement in the NNH portion of the GRI code since versions 2.11 with the release of version 3.0. More experimental work is needed to accurately model the formation of NO via NNH.[21] Even with discrepancies it is noted that the GRI 3.0 mechanism is improved in its ability to show the formation of NO from NNH. Using the GRI 3.0 mechanism to show relative reaction activity in a hydrogen fueled MTG compared to a natural gas fueled MTG would not quantitatively prove the level of NO being produced by NNH but give a strong qualitative comparison.

The GRI 3.0 mechanism was used to determine if the NNH reaction pathways were more sensitive during a hydrogen reaction than with a methane reaction. For each fuel type engine conditions of pressure 3.559atm, inlet temperature 832.75K and equivalence ratio 0.20 for hydrogen and 0.49 for methane were used. Initial reactor temperatures of 1000K, 1200K, 1400K and 1600K were investigated. Sensitivity values were taken at the point when 5-80% of the fuel was consumed.[22] After executing the code all reactions involving NNH or NO were extracted. The ten most sensitive reactions from each fuel were collected and plotted. The sensitivity results for methane can be seen in Figure 13 and for hydrogen in Figure 14. Table 4 lists the reactions found in Figure 13 and Figure 14. Reactions listed in red and bold are common to both methane and hydrogen reactions. Those reactions underlined are only found in the hydrogen reactions.

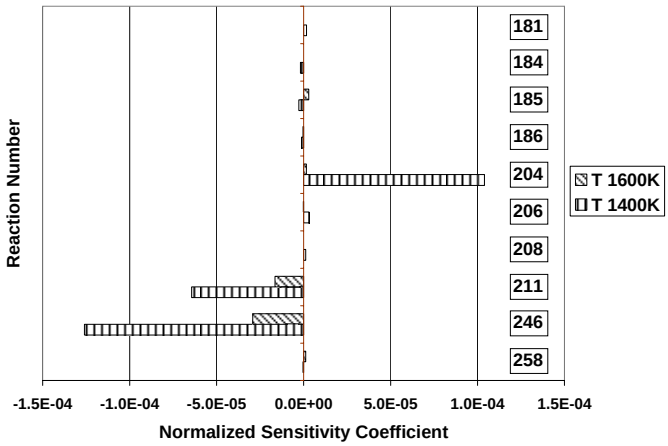

Figure 13: Normalized Sensitivity Coefficients for Methane. Run at Engine Inlet Conditions and Various Reactor Temperatures.

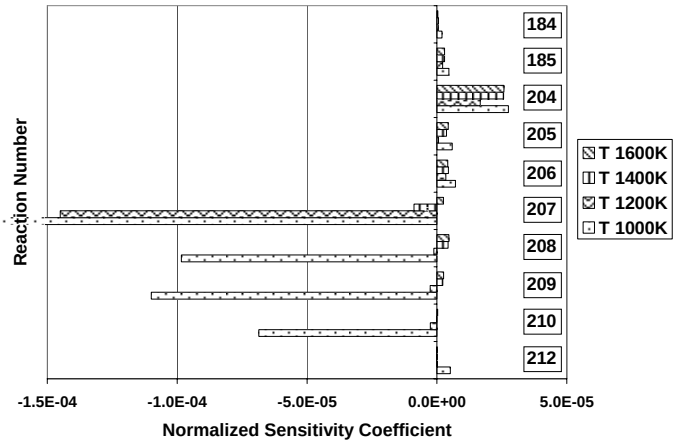

Figure 14: Normalized Sensitivity Coefficients for Hydrogen. Run at Engine Inlet Conditions and Various Reactor Temperatures.

Initial reactor temperatures of 1400K and 1600K only appear when methane is used as the fuel. At temperatures of 1000K and 1200K no methane reaction occurs. At an initial reactor temperature of 1400K methane shows great sensitivity to reactions 204, 211 and 246. Reaction 204 is driven in the forward reaction while 211 and 246 in the reverse. The reverse of reaction 211 leads to the formation of NNH while the forward 204 consumes the produced NNH forming monatomic hydrogen and diatomic nitrogen. Reaction 246 in the reverse direction directly forms NO from the intermediate HCN and O in no way participating in NO formation from NNH. Changing the initial temperature of the reactor to 1600K results in the same reactions being the most sensitive though less so in magnitude.

Table 4: Reaction Numbers and Statements. Taken from GRI 3.0[10]

#	Reaction	#	Reaction
181	$N2O+O \leftrightarrow N_2+O_2$	**208**	**$NNH+O \leftrightarrow NH+NO$**
184	**$N_2O+OH \leftrightarrow N_2+HO_2$**	209	$NNH+H \leftrightarrow H_2+N_2$
185	**$N_2O(+M) \leftrightarrow N_2+O(+M)$**	210	$NNH+OH \leftrightarrow H_2O+N_2$
186	$HO_2+NO \leftrightarrow NO_2+OH$	211	$NNH+CH_3 \leftrightarrow CH_4+N_2$
204	**$NNH \leftrightarrow N_2+H$**	212	$H+NO+M \leftrightarrow HNO+M$
205	$NNH+M \leftrightarrow N2+H+M$	246	$CH+NO \leftrightarrow HCN+O$
206	**$NNH+O_2 \leftrightarrow HO_2+N_2$**	258	$HCNN+O \leftrightarrow HCN+NO$
207	$NNH+O \leftrightarrow OH+N_2$		

The response of hydrogen was more varied than that of methane. When the reactor had an initial temperature of 1000K reactions 207, 208, 209 and 210 are found to be very sensitive in the reverse direction. These four reactions all lead to the formation of NNH when in the reverse direction. Reactions 204, 205 and 206 consume NNH but at low initial reactor temperature are considerably less sensitive than the four reactions mentioned before that are producing NNH. When initial reactor temperature increases to 1400K the same reactions still show sensitivity and form NNH yet as with methane to a much lesser degree. As the temperature is increased further to 1400K and 1600K the NNH forming reactions reverse and start consuming NNH.

Both methane and hydrogen show an affinity to produce NNH at lower initial reactor temperatures. This follows with the discussion in the introduction that NO produced via NNH is more viable at lower temperatures. Hydrogen does not require a large amount of energy to react and can maintain a reaction at very low temperatures due to its large flammability limit. This allows for a greater potential of NO formation from NNH with hydrogen at low equivalence ratios than fuels that cannot sustain such low reaction temperatures.

In addition to GRI 3.0 a specific hydrogen mechanism was used to investigate the potential effect of NNH on NO formation with hydrogen. The mechanism is a combination of work done by Li et al.[23] and Mueller et al.[22] It combines the hydrogen air reaction with all forms of NO_x formation pathways. The NO_x formation predictions the code generates have not been compared against any NO_x flame production data. The code is used none the less due to a lack of alternatives combined with the desire to have a counterpart to the GRI 3.0 tests.

The hydrogen specific code showed nearly no NO formation via NNH. The most active reactions were four to six orders of magnitude less active than what GRI 3.0 predicted. While this directly contradicts the idea that NO is being formed via NNH the lack of validation in the hydrogen specific code point to the need for a strong mechanism if modeling is to be used to predict NO emissions from hydrogen gas turbines.

Though not proven, the formation of NO via NNH may explain why all three injectors produced approximately 50ppm NO at a lean equivalence ratio of 0.20. The adiabatic flame temperature of hydrogen at an equivalence ratio of 0.20 is approximately 1400K which effectively eliminates any thermal NO. At higher power loads the higher adiabatic flame temperature indicates that NO formation via the Zel'dovich pathway should be dominant.

Dilute Combustion Analysis

The Capstone C60 operated on natural gas produces very little criteria pollutant emissions. Past studies of the engine show that, at full load, emissions of CO and NO corrected to 15% O_2 do not exceed 5.7ppm and 4.9ppm respectively.[8] These low emissions have been attributed to near perfect premixing of fuel and air along with ultra fuel lean equivalence ratios. Additionally the geometry of the engine and the flow conditions entering the combustion chamber may be leading to the low emission values.

A technique used to lower NO emissions from a combustor involves injecting partially combusted products that would contain NO into a fresh stream of fuel and oxidant. This paper will refer generally to this idea as dilute combustion though other unique names for the various configurations of combustors that use this principle exist.

This technique has been presented historically for different combustion technologies. The first application of this idea has been to furnaces. The first such furnace combustor was named a low NO_x regenerative burner.[24] This dilute combustion device used a diffusion pilot flame to create partially combusted gasses. These gasses were then fed directly into the reaction zone of a larger secondary diffusion reaction. The heat from the pilot flame preheated the incoming main air which in turn increased flame stability. By introducing the combusted gasses to the main reaction NO_x levels were reduced by 50% compared to traditional furnace burners.

Another furnace application[25] of dilute combution focused on the air preheat gains of exhaust gas recirculation. This study showed that burner configurations that directly interacted product gas with reaction zones reduced emission levels of both CO and NO_x. Additionally non-combustion product diluents N_2 and CO_2 were injected with the oxidant stream. While both diluents caused a reduction in reaction temperature the use of CO_2 created a larger reduction of criteria pollutants. This suggested that not only does the diluent effect lower emission levels through reaction temperature changes but the chemistry of the added diluent impacts emission levels.

The idea of using partially oxidized gasses to stabilize a reaction and reduce NOx emissions has been outlined for other combustors.[26] One type dubbed a "flameless oxidation combustor" due to the "invisible flame" it generates utilizes partially combusted products to reduce NO_x levels and stabilize the reaction. A distinction is made with exhaust gas recirculation which utilizes combusted products from the exhaust stack that are brought into the oxidant stream before combustion occurs. Instead, the flameless combustor recycles combustion products internally to the combustion chamber. In order to obtain a flameless oxidation reaction a "loop reactor" is necessary. The three loop reactors diagramed and reproduced in Figure 15 all incorporate a geometry that returns combustion product to the combustion zone.

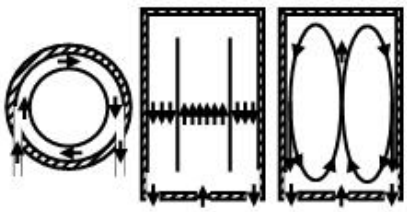

Figure 15: Diagram of "Loop Reactors" Presented for Flameless Oxidation[26]

The leftmost loop reactor diagram in Figure 15 uses nearly the same tangential injection and annular configuration as the Capstone C60. The concept of a burner that would utilize exhaust gas as a way to stabilize a reaction and reduce emissions has been proposed for a similar combustor geometry,[27] which is also similar to the left most loop reactor of Figure 15. As the reactants from one injector enter the combustor and begin the oxidation process traditionally modeled in plug flow reactors they are prematurely interrupted and encounter the relatively cool reactants from the second reactor. The combined partially combusted products from the first injector and fresh reactants from the second injector combine and react on their path to the first injector where fresh reactants wait to continue the process. This process is diagramed in Figure 16. A fraction of the combusted products enter a burnout zone and exit the combustor axially. There are two important requirements for this process to take place: A certain fraction of the combustion products must enter the fresh reactant stream and they must enter at the right time during the kinetic process.

The momentum of the flow field will dictate the transit of species from the injector, to their ignition, through the kinetic process and into the next injector's path. If the magnitude of momentum is not great enough the reacting fuel and air will not reach the second injector and simply be transported from the combustion chamber. Low momentum will result in the dilute combustion strategy not occurring.

Atmospheric testing of a dilute combustion system with similar geometry to the Capstone C60 has been reported.[28] The experimentation showed that the addition of partially oxidized gases could help stabilize a reaction of fresh reactants and decrease the lean blow out limit of a fuel. The combustor contained two injectors that could be adjusted to allow for different angles of injection into the combustor. As this angle was changed emissions of CO and NO_x changed as well. By changing this angle the residence time of the path from injector exit to the second injector can be manipulated. As this residence time increased and decreased with the injector angle the kinetic reaction-taking place had a longer or shorter period of time to be driven towards equilibrium. Optimization of the time a reaction is allowed to exist before introduction to the new reactant stream can maximize the NO mitigation potential. This optimization led to sub ppm levels of NO_x and CO in the combustor tested when operated on natural gas.

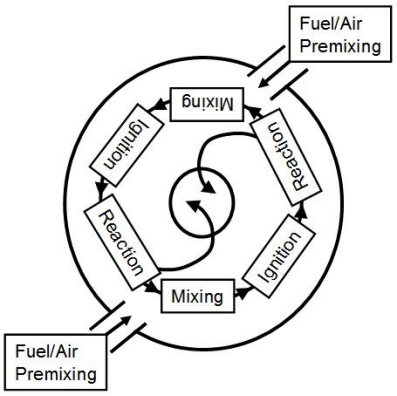

Figure 16: Recreated NO_x Reburn Engine Pathways Diagram[27]

This strategy of a dilute combustion engine using partially combusted products combining with fresh reactants to produce low emissions has been proven through experimentation.[29,30]

The stagnation point reverse flow type combustor injects fuel and air from an open end of a tube towards a closed end. This combustor geometry is analogous to the right most diagramed loop reactor described for flameless oxidation reprinted in Figure 15. The reacting fuel and air entering the chamber are sheared by the partially combusted products returning from the stagnation plane at the other end of the tube. This shearing effect and combination of partially combusted products along with fresh reactants resulted in low emissions of CO and NO_x.

The chemistry behind dilute combustion has been investigated.[31] A counter-flow laminar flat flame burner was used to determine the effect of different diluents on emission levels of NO. Varying amounts of CO_2, N_2 and burned gas containing NO were injected to the oxidant inlet stream. Reductions in the output levels of NO were seen when diluents CO_2 and N_2 were added to the oxidant stream. The effect of adding these species lowered the reaction temperature and reduced thermal NO_x production. When NO laden burned-gas was introduced to the oxidant stream the initial concentration of NO increased but post combustion the amount of NO was lower than before combustion. The introduction of NO to the combustion region was shown to reduce the amount of NO that would have been produced without diluent. Kinetic modeling of the reaction showed a considerable increase of N_2 production from N and as well as NO destruction when burned gas was used for dilution. NO destruction reactions are listed that are of primary importance when burned gas is present added to a reaction.

The Capstone C60 contains a geometry that may be promoting dilute combustion when operated with natural gas. Modification to the injector hardware did not affect the effectiveness of this strategy when fueled with natural gas as seen in Figure 10. Changing fuel stocks from natural gas to hydrogen does not affect the momentum in the engine. This constant momentum coupled with the greatly differing reaction rates may be giving rise to mismatched time scales associated with the mixing, ignition, and reaction zones. Additionally the time necessary to drive a hydrogen reaction to equilibrium is considerably less than that of natural gas. This time difference is shown in Figure 12. With the preclusion of NO_x reburn due to the change from natural gas to hydrogen NO emissions generated in the engine could increase.

CONCLUSIONS

Multiple modifications to the fuel injectors of a commercial natural gas fired MTG have been made so allow the engine to operate on pure hydrogen. These modifications created three unique fuel/air mixing profiles while maintaining similar equivalence operational ranges. The injectors were characterized in an atmospheric test rig for their mixing profiles. Emission performance of each injector type was tested in an MTG over its full range. Each injector type was tested four times. The data gathered from the engine was compared to power load, equivalence ratio and mixing level. Emission levels dropped as the mixing profile of the injector became more uniform. Lower equivalence ratios uniformly produced less NO.

Compared to natural gas operation the engine run on hydrogen produced larger volumes of NO. This follows the precedent set by previous work when engines are retrofitted to operate with hydrogen. Four potential effects that would lead to higher NO emissions from the engine when fueled with hydrogen are presented.

- The control strategy of the MTG is not optimized for hydrogen and is causing a large volume of thermal NO production in the combustor at full load.
- Residence time analysis was conducted for hydrogen at multiple equivalence ratios. By utilizing lower equivalence ratios along with early termination of the reaction emissions of NO could be reduced.
- Kinetics modeling of NO formation was conducted. Specifically the residence time of combustible species at engine conditions was examined to see the rate of formation of NO. NO formation is much slower when methane is used as a fuel stock compared to hydrogen. By lowering the equivalence ratio of hydrogen a similar NO formation rate to that of methane can be obtained. Sensitivity studies were conducted to examine the roll of NNH in the production of NO. Hydrogen showed a greater affinity to produce NO via the NNH formation route when modeled with the GRI 3.0 mechanism. NO is more likely to be produced at lower temperatures via NNH than at higher temperatures. Hydrogen at low equivalence ratios has a low adiabatic flame temperature conducive to NO being formed by NNH.
- The concept of dilute combustion in the commercial natural gas Capstone C60 may be leading to the engine's low emission values when operating with natural gas. When the fuel type is changed to hydrogen without changing the combustor geometry dilution may not be occurring. This could lead to the increase in NO seen.

ACKNOWLEDGMENTS

The support of the California Energy Commission (Contract 500-00-020) is gratefully acknowledged. The support of Richard Hack and discussions with Mark Mitchell of Capstone Turbine Corporation are appreciated.

REFERENCES

[1] Lefebvre, A.H., 1999, *Gas Turbine Combustion (2nd Ed.)*, Philadelphia, PA, Taylor and Francis

[2] Effinger, M.W., Mauzey, J.L., and McDonell, V.G, 2005, "Characterization and Reduction of Pollutant Emissions from a Landfill and Digester Gas Fired Microturbine Generator," Paper GT2005-68520, ASME Turbo Expo, Reno, NV.

[3] Conrad, W.E., and Corrington, L.C., 1957, "NACA Research Memorandum: Hydrogen for Turbojet and Ramjet Powered Flight," NACA RM E57D23

[4] Nomura, M., Tamaki, H., Morishita, T., Ikeda, H., and Hatori, K., 1981, "Hydrogen Combustion Test in a Small Gas Turbine," *International Journal of Hydrogen Energy*, Vol. 6 (4), pp 397-412
[5] Sampath, P., and Shum, F., 1985, "Combustion Performance of Hydrogen in a Small Gas Turbine Combustor," *International Journal of Hydrogen Energy*, Vol. 10 (2), pp 829-837
[6] Chiesa, P., Lozza, G., Mazzocchi, L., 2005, "Using Hydrogen as Gas Turbine Fuel" *J. Engr. Gas Turbines and Power*, Vol. 127, pp, 73-80
[7] Therkelsen, P.L., Mauzey, J.L., McDonell, V.G., and Samuelsen, S., 2006, "Evaluation of a Low Emission Gas Turbine Operated on Hydrogen," Paper GT2006-90725, ASME Turbo Expo, Barcelona, Spain, May.
[8] Phi, V.M., Mauzey, J.L., McDonell, V.G., and Samuelsen, G.S., 2004, "Fuel Injection and Emissions Characteristics of a Commercial Microturbine Generator," Paper GT2004-54039, ASME Turbo Expo, Vienna, Austria, June.
[9] Reaction Design, 2006, Chemkin Version 4.0.2
[10] GRI-Mech 3.0, http://www.me.berkeley.edu/gri_mech/
[11] Konnov, A.A., Dyakov, I.V., De Ruyck, J., 2002, "Nitric Oxide Formation in Premixed Flames of H_2 + CO + CO2 and Air," *Proceedings of the Combustion Institute*, Vol. 29, pp 2171-2177
[12] Mueller, M.A., Kim, T.J., Yetter, R.A., and Dryer, F.L., 1999, "Flow Reactor Studies and Kinetic Modeling of the H_2/O_2 Reaction," *International Journal of Chemical Kinetics*, Vol. 31 (2), pp 113-125
[13] Reed. R.J, 1985, North American Combustion Handbook, Vol 1, 3rd edition, North American Mfg. Co.
[14] Miller, J.A., Branch, M.C., and Kee, R.J., 1981, "A Chemical Kinetic Model for the Selective Reduction of Nitric Oxide by Ammonia," *Combustion and Flame*, Vol. 43, pp 81-98.
[15] Bozzelli, J.W., and Dean, A.M., 1995, "O + NNH: A Possible New Route for NO_x Formation in Flames," *International Journal of Chemical Kinetics*, Vol. 27, pp 1097-1109
[16] Konnov, A.A., Colson, G., De Ruyck, J., 2001, "NO Formation Rates for Hydrogen Combustion in Stirred Reactors," *Fuel*, Vol. 80, pp 49-65
[17] Hayhurst, A.N., Hutchinson, E.M., 1998, "Evidence for a New Way of Producing NO via NNH in Fuel-Rich Flames as Atmospheric Pressure," *Combustion and Flame*, Vol. 114, pp 274-279
[18] Baulch, D.L., Cobos, C.J., Cox, R.A., Esser, C., Frank, P., Just, Th., Kerr, J.A., Pilling, M.J., Troe, J., Walker, R.W., and Warnatz, J.J. 1992, "Evaluated Kinetic Data for Combustion Modeling," *Journal of Physics and Chemical Reference*, Vol. 21(3), pp 411-734
[19] Michael, J.V., and Lim, K.P. 1992, "Rate Constants for the N_2O Reaction System: Thermal Decomposition of N_2O; N+NO → N_2 + O; and Implications for O + N_2 → NO + N," *Journal of Chemical Physics*, Vol. 97(5), pp 3228-8234
[20] Charlston-Goch, D., Chadwick, B.L., Morrison, R.J.S., Campisi, A., Thomesn, D.D., and Laurendeau, N.M., 2001, "Laser-Induced Fluorescence Measurements and Modeling of Nitric Oxide Premixed Flames of CO + H_2 + CH_4 and Air at High Pressures," *Combustion and Flame*, Vol. 125, pp 729-743
[21] Hughes, K.J., Tomlin, A.S., Hampartsoumain, E., Nimmo, W., Zsely, I.G., Ujvari, M., Turanyi, T., Glague, A.R., and Pilling, M.J., 2001, "An Investigation of Important Gas-Phase Reactions of Nitrogenous Species from the Simulation of Experimental Measurements in Combustion Systems", *Combustion and Flame*, Vol. 124, pp 573-589
[22] Mueller, M.A., Yetter, R.A., Dryer, F.L., 2000, "Kinetic Modeling of the $CO/H_2O/O_2/NO/SO_2$ System: Implications for High-Pressure Fall-off In the SO_2 + O(+M) = SO_3(+M) Reaction," *International Journal of Chemical Kinetics*, Vol. 32(6), pp 317-339
[23] Li, J., Zhao, Z., Kazakov, A., and Dryer, F.L., 2004, "An Updated Comprehensive Kinetic Model of Hydrogen Combustion," *International Journal of Chemical Kinetics*, Vol. 36 (10), pp 566-575
[24] Suzukawa, Y., Sugiyama, S., Hino, Y., Ishioka, M., and Mori, I., 1997, "Heat Transfer Improvement and NO_x Reduction by Highly Preheated Air Combustion," *Energy Conversion Management*, Vol. 38 (10-13), pp 1061-1071
[25] Hasegawa, T., Tanaka, R., and Niloka, T., 1997, "High Temperature Air Combustion Contributing to Energy Saving and Pllutnat Reduction in Industrial Furnace," International Joint Power Generation Conference, Vol. 1, pp 259-266
[26] Wünning, J.A., and Wünning, J.G., 1997, "Flameless Oxidation to Reduce Thermal NO-Formation," *Progress in Energy and Combustion Science*, Vol. 23, pp 81-94
[27] Kalb, J.R., and Sattelmayer, T., 2004, "Lean Blowout Limit and NO_x Production of a Premixed Sub-ppm NO_x Burner with Periodic Flue Gas Recirculation," Paper GT2004-53410, ASM Turbo Expo, Vienna, Austria, June.
[28] Brückner-Kalb, J.R., Hirsch, C., Sattelmayer, T., 2006, "Operation Characteristics of a Premixed Sub-ppm NO_x Burner with Periodical Recirculation of Combustion Products," Paper GT2006-90072, Barcelona, Spain, May.
[29] Neumerier, Y., Weksler, Y., Zinn, B., Seitzman, J., Jagoda, J., and Kenny, J., 2005, "Ultra Low Emissions Combustor with Non-Premixed Reactants Injection," Paper AIAA-2005-3775, 41st AIAA/ASME/SAE/ASEE Joint Propulsion Conference, Tuscon, AZ, July.
[30] Bobba, M.K., Gopalakrishna, P., Seitzman, J.M., and Zinn, B.T., 2006, "Characteristics of Combustion Processes in a Stagnation Point Reverse Flow Combustor," Paper GT2006-91217, ASEM Turbo Expo, Barcelona, Spain, May.
[31] Choi, G.-M., Katsuki, M., 2002, "Chemical Kinetic Study on the Reduction of Nitric Oxide in Highly Preheated Air Combustion," *Proceedings of the Combustion Institute*, Vol. 29, pp 1165-1171

